AP1000® PWR REACTOR PHYSICS ANALYSIS WITH VERA-CS AND KENO-VI - PART II: POWER DISTRIBUTION

F. Franceschini
Westinghouse Electric Co. LLC,
Cranberry Township, Pennsylvania, USA
francef@westinghouse.com

A. T. Godfrey, J. C. Gehin
Oak Ridge National Laboratory
godfreyat@ornl.gov

ABSTRACT

Westinghouse has applied the Core Simulator of the Virtual Environment for Reactor Applications, VERA-CS, under development by the Consortium for Advanced Simulation of LWRs (CASL) to the core physics analysis of the **AP1000**® PWR. The **AP1000** PWR features an advanced first core with radial and axial heterogeneities, including enrichment zoning, multiple burnable absorbers, and a combination of light and heavy control banks to enable the MSHIM™ advanced operational strategy. These advanced features make application of VERA-CS to the **AP1000** PWR first core especially relevant to qualify VERA performance. A companion paper at this conference describes the results obtained with VERA-CS and the KENO Monte-Carlo code for startup physics tests simulations of the **AP1000** PWR first core (critical boron, rod worth and reactivity coefficients). This paper describes the results of detailed power distribution comparisons between VERA-CS and KENO, and confirms the excellent numerical agreement reported in the companion paper for the startup physics tests simulations.

Key Words: **AP1000, PWR, VERA, CASL, KENO**

1 INTRODUCTION

The **AP1000** PWR features a low-leakage 18-month cycle advanced first core, with five fuel regions, intra-assembly enrichment zoning, and a combination of burnable absorbers: the Westinghouse Integral Fuel Burnable Absorber (IFBA), a ZrB_2 coating on the pellet surface, and the Wet Annular Burnable Absorber (WABA), an insert employed at selected guide thimble locations [1]. Gray tungsten and standard Ag-In-Cd control banks are employed for MSHIM™, an advanced operational strategy that provides robust core reactivity and axial power distribution control with minimal changes to the soluble boron concentration during both normal operation and power maneuvers[2],[3]. These advanced features make application of the VERA Core Simulator (VERA-CS) under development by CASL to the **AP1000** first core especially relevant to qualify its performance.

An extensive set of simulations has been performed throughout this activity. A companion paper at this conference presents the results obtained for calculations that support Zero Power Physics

AP1000® and MSHIM™ are trademarks or registered trademarks of Westinghouse Electric Company LLC in the United States and may be registered in other countries throughout the world. All rights reserved. Unauthorized use is strictly prohibited.

CASL-U-2015-0006-000

Tests (ZPPTs), and in particular the all-rods-out critical boron concentration, control rod worth and reactivity coefficients [4].

The results presented here are focused on the analysis of the power distribution results from VERA-CS simulations. In particular, simulations pertaining to the geometry below have been performed and the results are reported here:

- 2D lattice and multi-lattice calculations up to a core radial slice
- 3D assembly calculations up to a 3x3 partially controlled configuration

The geometry and fuel configurations analyzed are representative of the **AP1000** PWR first core and MSHIM operation. A detailed description of the **AP1000** PWR first core, including the modeling approach, can be found in the companion paper [4].

As for the ZPPT simulations, these simulations have been performed for the start-up core at Hot Zero Power (HZP) where given the fresh fuel and uniform temperature conditions it is possible to establish Monte-Carlo Continuous Energy reference solutions for the numerical validation of the VERA results.

The VERA solutions employ the SP_5 solver with P_3 scattering in 23 energy groups and on-the-fly pin-homogenized cross-sections generated from a 252-group ENDF/B-VII.0 SCALE library [4]-[9]. The Monte Carlo simulations have been performed using the Monte Carlo criticality code KENO-VI ([10]) with parallel transport capabilities and using continuous energy (CE) energy treatment [11]. The KENO simulations rely on an ENDF/B-VII.0 CE cross section library generated by the AMPX code system ([12]) at the HZP temperature of 565 K. Due to the rigorous neutron transport and energy treatment of CE Monte Carlo, the KENO results are assumed as the numerical reference throughout this paper. An application of the VERA and KENO-VI package to the startup core analysis of a commercial PWR which includes validation against plant measurements is given in [13] and [14].

2 RESULTS

2.1 2D Lattice Results

2D lattice results for VERA and KENO for the lattice types characterizing the **AP1000** PWR first core are summarized in Table 1. Note that there are twenty lattice types in this first core, as it derives by the adoption in the core design of five fresh-fuel regions (1 to 5 in Table 1) with various intra-assembly loading patterns, for a total of seven assembly types (1 to 4 and 5A, 5B, 5C in Table 1), which considering the axial heterogeneities of some assemblies leads to twenty uncontrolled lattice types.

Regions 1 and 2 feature respectively natural U and 1.58 w/o ^{235}U enrichment, uniform radially within the lattice and constant axially along the fuel stack, thus resulting into two lattice types (Lattice # 1 and 2 in Table 1). Region 3 features radially uniform 3.2 w/o ^{235}U enrichment in the central region of the fuel stack with 1.58 w/o ^{235}U top and bottom solid axial blankets (Lattice # 2 and 4).

Region 4 features radial enrichment zoning, with average enrichments of ~3.8 ^{235}U, in the central

region of the fuel stack and uniform 3.2 w/o ^{235}U top and bottom axial blankets. The Westinghouse Integral Fuel Burnable Absorber (IFBA) ZrB_2 coating and the Wet Annular Burnable Absorber (WABA) discrete annular inserts are also employed. In particular IFBA is present in 68 fuel rods and used in the central region of the stack, while annular blankets accommodate the higher helium content generated in neutron reactions with ^{10}B in ZrB_2. The 12 WABA inserts are positioned with the tip 8-in from the bottom of the active fuel, and the ^{10}B bearing portion offset downward with respect to the axial midline. Eight of the twelve WABA rods ("Short WABA") also feature an unpoisoned 15-in bottom Zr spacer and a top 43-in plenum. The remaining four WABA rods ("Long WABA") are poisoned except for the top 8-in plenum. As a result of the axial heterogeneities in the WABA inserts and due to the presence of the blankets, there are in total 5 lattice types in Region 4 (Lattice #5 to 9 in Table 1).

Region 5 has similar features to Region 4 but higher enrichment, ~4.4 vs. ~3.8 w/o ^{235}U on average in the central region of the fuel stack. Three assembly types pertain to Region 5: 5A with 88 IFBA rods and 4 WABA inserts, 5B with 124 IFBA rods and no WABA inserts, and 5C with 124 IFBA rods and 12 WABA inserts. The WABA inserts in Region 5 have a ^{10}B bearing central portion of 116 in, intermediate between the 102-in and 152-in of the Short and Long WABA in Region 4. As a result of the three assembly types, axial WABA heterogeneities and axial blankets, a total of 11 different lattice types (Lattice # 10 to 20) are found in Region 5.

The comparison of reactivity and power† distribution for VERA-CS vs. KENO for these 20 lattice types is given in Table 1. The leftmost column indicates the assembly type of pertinence for each lattice, while the "Case ID" column contains a succinct description of the lattice configuration. The table then shows the reference k_{inf} from CE KENO calculations and the difference in pcm (per cent mille) between VERA-CS and KENO. The two rightmost columns summarize the agreement in power distribution for VERA-CS vs. KENO, using two representative parameters: "ΔP RMS", that is the root mean square (RMS) of the power difference (VERA-KENO) weighted by the fuel rod volumes of a given lattice and the maximum absolute difference "ΔP Max". The delta in k_{inf} is also plotted in Figure 1, while the RMS and Max ΔP are plotted in Figure 2

The reactivity prediction from VERA-CS is in excellent agreement with CE KENO at HZP conditions, with an average difference of -34 pcm and a standard deviation of ~40 pcm. The slightly lower reactivity prediction for VERA-CS is confirmed in 3D core calculations reported in the companion paper [4], with ~-30 pcm 3D core delta k_{eff} for VERA vs. KENO at HZP All-Rods-Out conditions.

Lower enrichment lattices, especially natural U, are less reactive in VERA-CS than in KENO, while at higher enrichment without zoning the agreement becomes virtually perfect. Enrichment zoning, and/or use of IFBA, seems to slightly deteriorate the agreement, with some favorable compensation of errors from localized strong absorbers (e.g. WABA). These biases are however small.

VERA-CS agrees well with KENO also in the power distribution prediction showing only a mild deterioration for localized strong absorbers, IFBA, and enrichment zoning lattices. The delta power RMS across all lattice types simulated is ~0.2%, with a maximum absolute delta power of ~0.6% and ~0.4% on average.

† Comparisons actually used fission rates, however the term "power" instead of "normalized fission rate" is used for brevity in this paper.

Table 1 Lattice results

			KENO	VERA-CS		
Assembly ID	**Case#**	**Case ID**	k_{inf} (±3 pcm)	Δk_{inf} (pcm)	ΔP RMS (%)	ΔP Max (%)
1	1	^{235}U @ 0.74	0.66846	-102	0.13	0.30
2	2	^{235}U @ 1.58	0.95127	-38	0.15	0.31
3	3	^{235}U@ 3.20	1.18998	-7	0.19	0.40
3	4	^{235}U@ 1.58 (BLKT)	0.95226	-21	0.15	0.27
4	5	^{235}U@ 3.78 - 68 IFBA 12WB	1.03710	28	0.25	0.58
4	6	^{235}U@ 3.78 - 68 IFBA 8WB-4ZR	1.06471	61	0.25	0.60
4	7	^{235}U@ 3.78 - 68 IFBA 8WB-4TP	1.06583	-5	0.25	0.54
4	8	^{235}U@ 3.20 - 68 IFBA 12TP	1.18570	-14	0.23	0.40
4	9	^{235}U@ 3.20 (BLKT, 68 ANLR, 12TP)	1.18525	-10	0.24	0.42
5A	10	^{235}U@ 4.38 - 88 IFBA 4 WB	1.12083	-46	0.26	0.49
5A	11	^{235}U@ 4.38 - 88 IFBA 4 ZR	1.14851	-39	0.24	0.52
5A	12	^{235}U@ 4.38 - 88 IFBA 4 TP	1.14997	-65	0.24	0.51
5A	13	^{235}U@ 3.20 - 88 IFBA 4TP	1.18379	-26	0.24	0.42
5A	14	^{235}U@ 3.20 (BLKT, 88 ANLR, 4TP)	1.18348	-12	0.23	0.42
5B	15	^{235}U@4.38 124 IFBA	1.10339	-106	0.25	0.58
5B/C	16	^{235}U@ 3.20 (BLKT, 124 ANLR)	1.18063	-43	0.28	0.55
5C	17	^{235}U@ 4.38 - 124 IFBA 8 WB	1.04637	-36	0.28	0.50
5C	18	^{235}U@ 4.38 - 124 IFBA 8 TP	1.10191	-90	0.25	0.55
5C	19	^{235}U@ 4.38 - 124 IFBA 8 ZR	1.10025	-70	0.25	0.56
5C	20	^{235}U@ 3.20 (BLKT, 124 ANLR, 8TP)	1.18086	-32	0.26	0.48
			Average	-34	0.22	0.45
			Standard Deviation	40		

Notes: BLKT stands for solid blanket, ANLR stands for annular blanket, WB stands for WABA, ZR indicates the presence of Zr-spacers in selected WABA rods, TP indicates the unpoisoned He-filled top of the WABA rod. The enrichment reported for Reg. 4 and Reg. 5 is the average lattice enrichment (enrichment zoning is used for these regions, with ^{235}U at 3.4, 3.8 and 4.2 w/o for Reg. 4 and ^{235}U at 4.0, 4.4 and 4.8 for Reg. 5). There is no enrichment zoning in Reg. 1 to 3. Δk is the delta reactivity VERA-CS vs. KENO in pcm, calculated as 10^5*Ln ($k_{VERA\text{-}CS}/k_{KENO}$). ΔP is the difference in normalized fission rate VERA-CS- KENO multiplied by 100, with ΔP RMS calculated as the root mean square of the differences and ΔP Max as the maximum absolute difference.

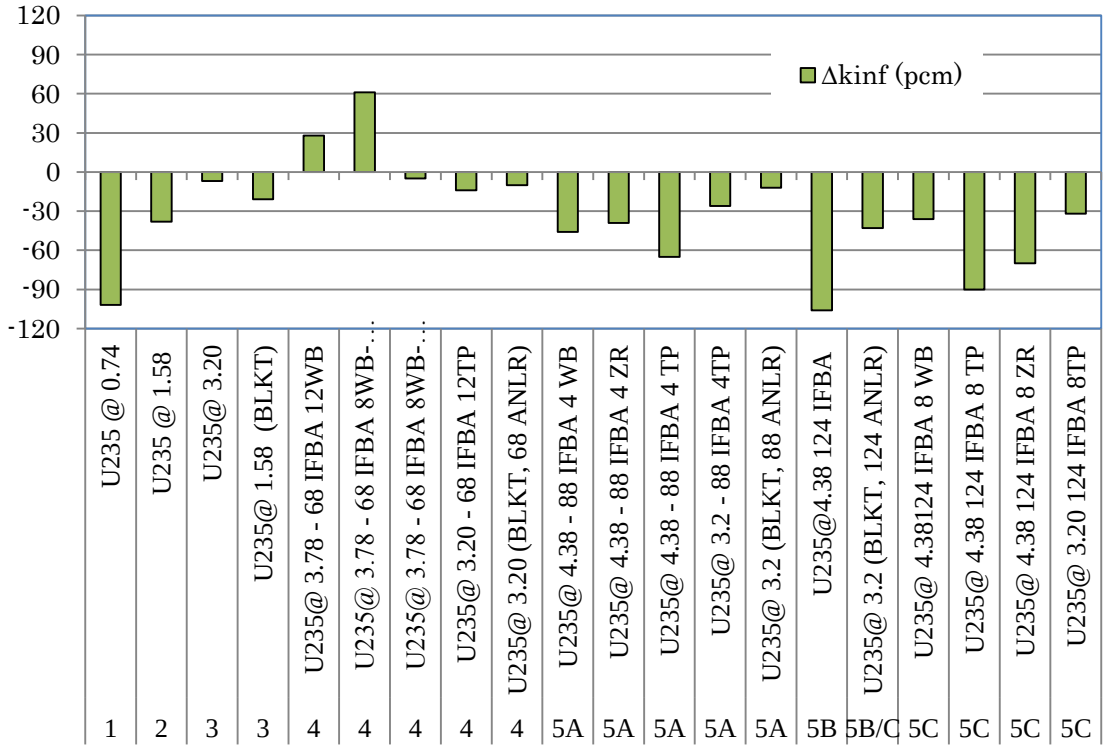

Figure 1 Delta k-inf VERA-CS-KENO (pcm) for 2D lattice simulations

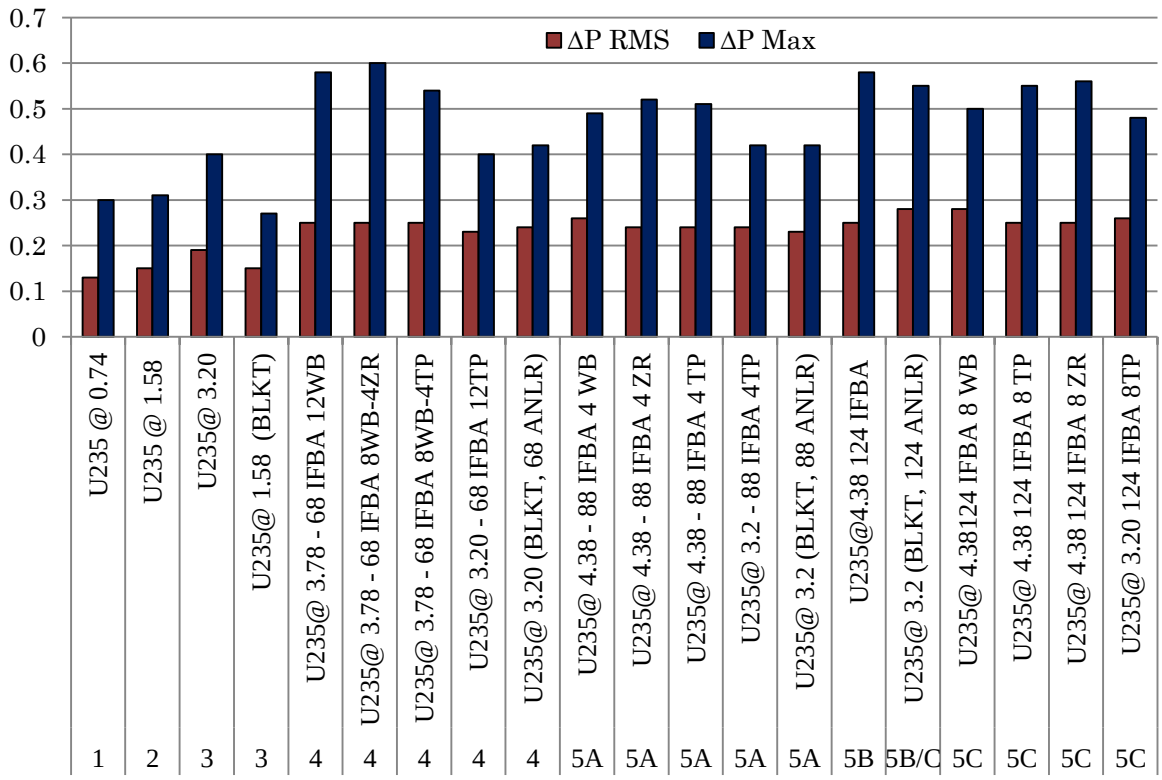

Figure 2 ΔP (RMS and Max) VERA-KENO for 2D lattice simulations

2.2 2D Multi-Lattice

The results of multi-lattice simulations are reported in Table 2. The geometry adopted is a 3x3 multi-lattice configuration mimicking the center of the **AP1000** PWR core at the axial midplane, as shown in Figure 3. In addition to an "unrodded" simulation, one simulation with Ag-In-Cd (black) control rods inserted in the central lattice of the 3x3 and one with tungsten (gray) control rods inserted in the central lattice have been performed. The k_{inf} predicted by VERA is ~-20 to -40 pcm from KENO, consistent with the single lattice results. The power distribution comparison is slightly worse than for single lattice cases but still satisfactory, with pin cell RMS <0.4% and Max <1%. This includes rodded cases which present specific challenges due to the local power suppression in the rodded assembly and power redistribution to the other assemblies. This good agreement is confirmed also at the assembly-interface locations, which may be challenging for these methods due to the impact of asymmetric spectral conditions. A slight deterioration of the agreement in the locations adjacent to one or more strong localized absorbers (e.g. control rods or WABAs) is noted but the resulting discrepancy is still below 1%.

Table 2 Multi-lattice results

	KENO		VERA-CS				
Case	SB (ppm)	K_{inf} (± 2pcm)	ΔK_{inf} (pcm)	RMS ΔP Lattice (%)	Max ΔP Lattice (%)	RMS ΔP Cell (%)	Max ΔP Cell (%)
Unrodded	1244	1.00199	-37	0.20	0.24	0.31	0.82
Ag-In-Cd	955	1.00235	-47	0.24	0.53	0.36	0.98
Tungsten	1130	1.00227	-19	0.21	0.31	0.32	0.89

SB: Soluble Boron. KENO uncertainties given in Table 6.

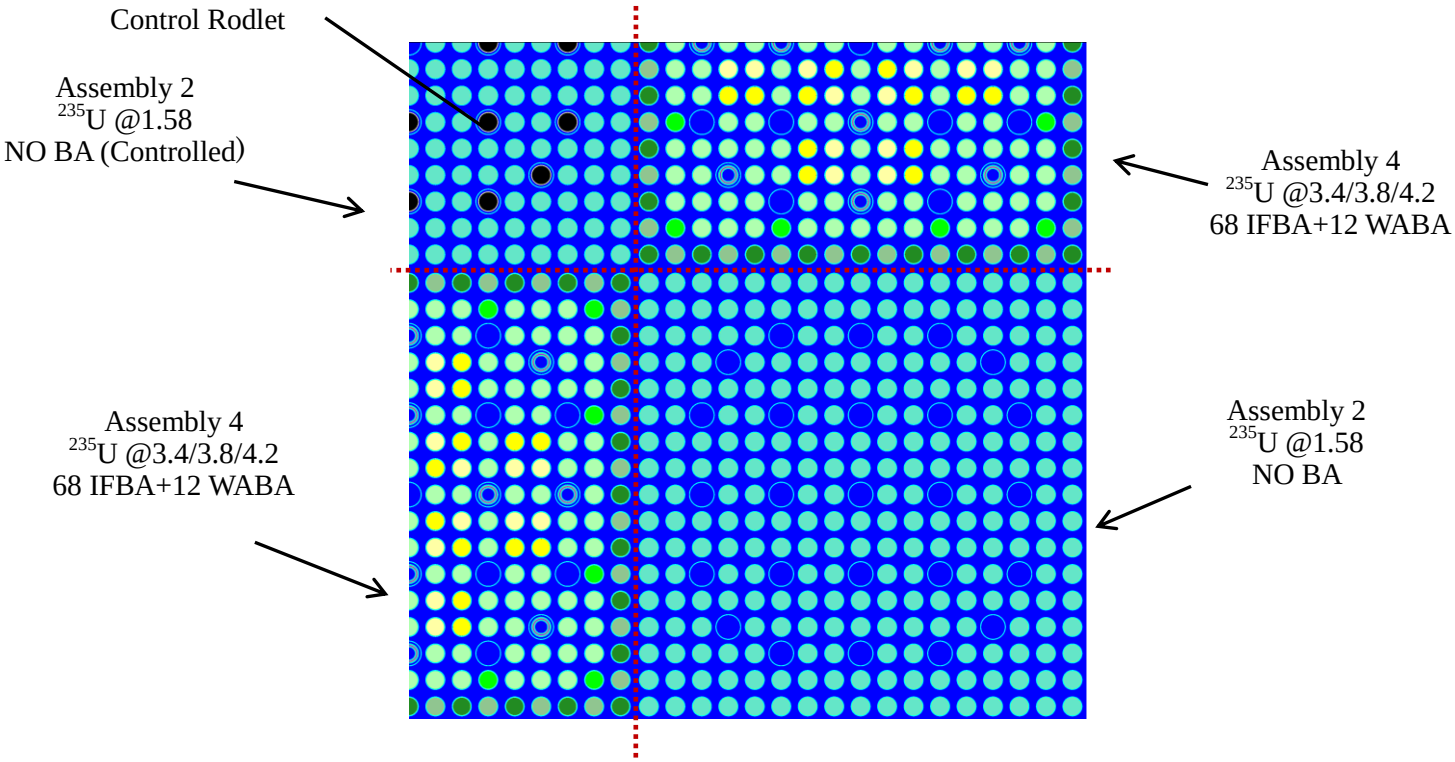

Figure 3 Loading Pattern for Multi-Lattice Simulations (rodded, quarter geometry)

2.3 Radial Core Slice

The results summarized in Table 3 refer to a radial core slice, including the reflector, at the core axial mid-plane of the core. The reflector consists of a 1-in stainless steel baffle surrounded by water. The geometry and loading pattern are displayed in Figure 4 together with a plot of the resulting KENO pin power distribution. The pin power comparison for VERA-CS vs. KENO is given on the left-hand side map of Figure 5, with the form factor‡ comparison on the right hand-side map.

Table 3 Summary comparison for core radial slice at the axial midplane

KENO	**VERA-CS**					
K_{inf} (± 1 pcm)	Δk_{inf} (pcm)	RMS ΔP Assembly (%)	Max ΔP Assembly (%)	RMS ΔP Pin (%)	ΔP Hot Pin (%)	Max ΔP Pin (%)
1.00097	0	0.21	0.42	0.39	0.78	3.1

Notes: coolant soluble boron of 1316 ppm. "Hot pin" is the pin with the highest relative power in the simulation. "Max assembly" and "Max pin" refer to the largest absolute difference VERA-KENO in respectively assembly and pin power predictions. KENO uncertainties given in Table 6.

The agreement between VERA-CS and KENO for this 2D core geometry is remarkable, as for the lattice and multi-lattice simulations. The eigenvalue prediction is virtually identical. The power distribution analysis shows delta assembly power RMS of 0.2% and delta pin power RMS of ~0.4% between VERA and KENO. The delta power for the "hot" pin, the pin with the highest relative power in the simulation, is 0.8%.

The ~3.0% maximum difference in the pin power prediction occurs in the very low power pins at the edge, and especially corners, of the core (red color locations in Figure 5). This is possibly caused by the strong asymmetry in the local spectral conditions for these pins compared to the reflective conditions assumed for the XSProc cross section collapsing step prior to performing the SP_N calculation [4],[6]. This is confirmed analyzing the delta pin form factors§ for VERA-CS vs. KENO shown on the map at the right hand side of Figure 5. This plot, in addition to the pins at the edge of the core, show other locations where the simple geometry assumed in the first energy collapsing step may lead to inaccuracies, e.g. at the interface, and especially corners, of the natural U assemblies with the neighboring higher-enriched assemblies. It should be noted that these fuel locations have very low power and belong to assemblies that are typically discharged at the end of the cycle.

‡ The form factors are the pin powers of a given assembly normalized by the power of the assembly. The normalization step effectively takes away any potential bias deriving from differences in the assembly power prediction between two codes, thus facilitating the analysis of the intra-assembly power shape prediction.

§ The form factors are the pin powers of a given assembly normalized by the power of the assembly. The normalization step effectively takes away any potential bias deriving from differences in the assembly power prediction between two codes, thus facilitating the analysis of the intra-assembly power shape prediction.

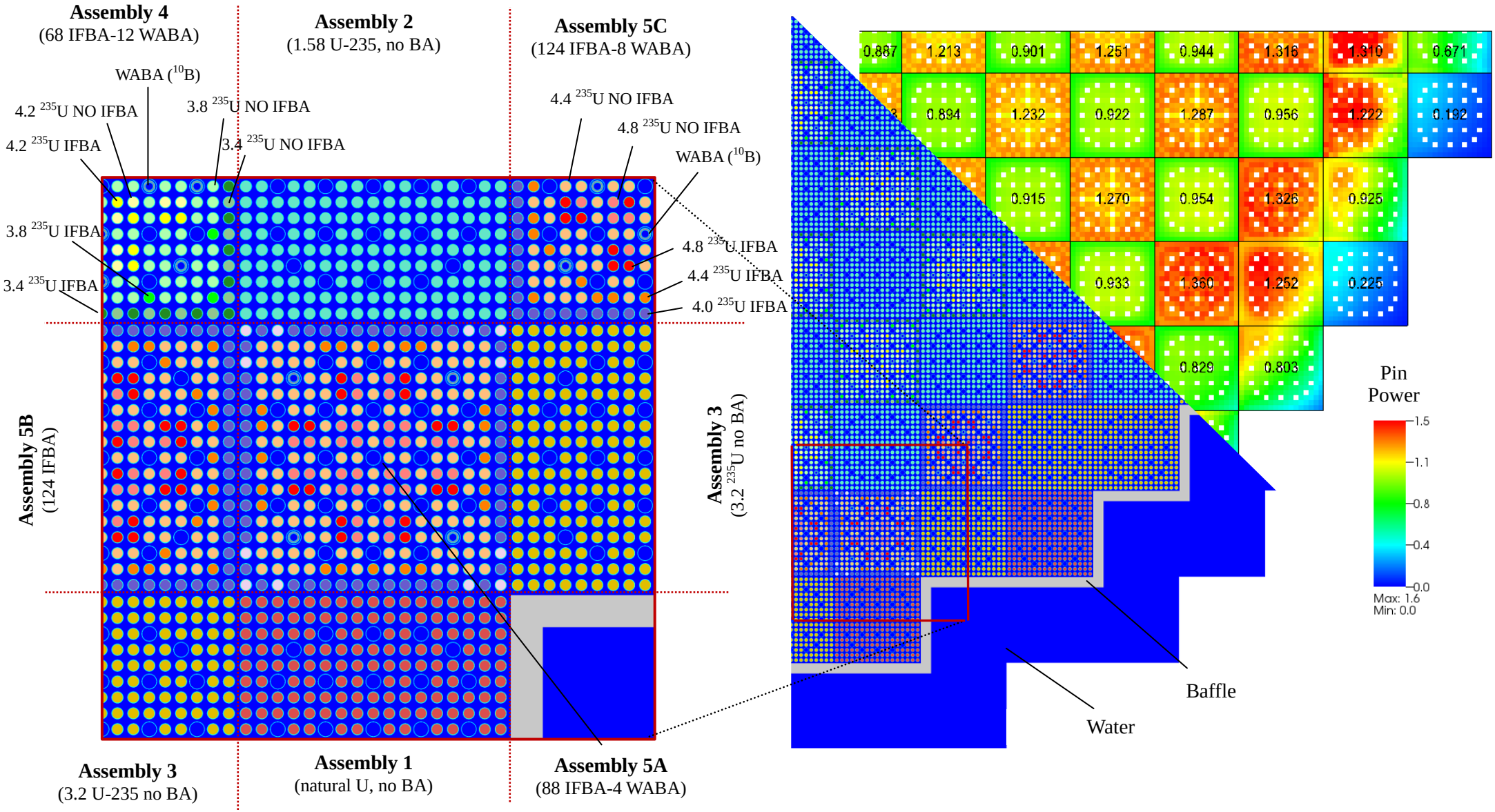

Figure 4 Radial core slice loading pattern and KENO pin power (octant geometry shown)

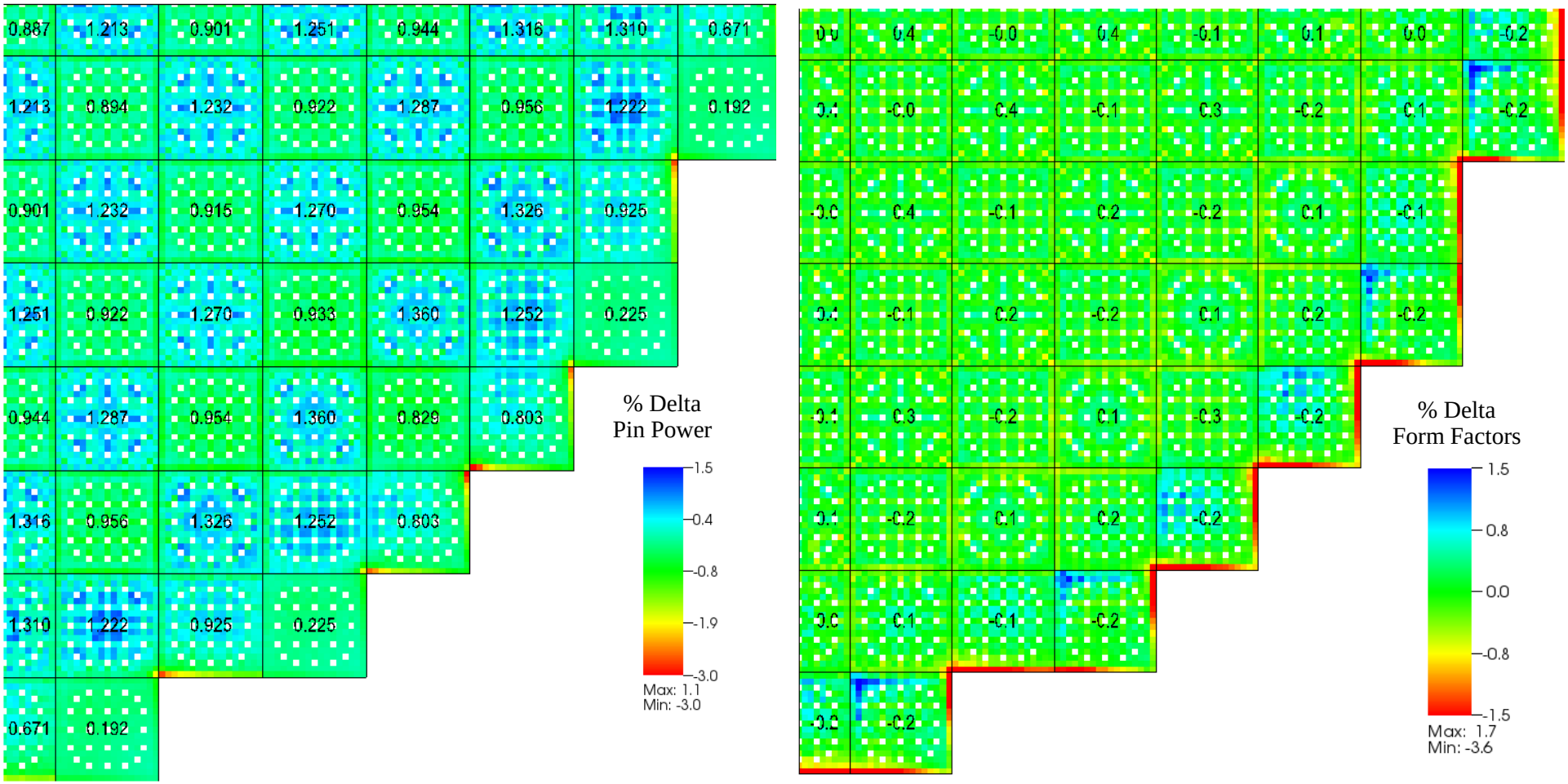

Figure 5 2D core delta pin power VERA-KENO (%, left) and delta form factor VERA-KENO (%, right)
(the numbers on the left map show the relative assembly power, % delta assembly power shown on the right map)

9 / 21

2.4 3D Assembly

3D calculations have been performed with VERA and KENO for each of the assembly types in the **AP1000** PWR first core. These simulations rely on a detailed representation of the fuel stack, including the structure comprised within the bottom and top core plates. The KENO model for assembly type 4 is shown in Figure 6 for the sake of illustration.

More specifically, the model contains explicit representation of the fuel rod stack, plenum, and end plugs, including solid and annular axial blanket regions. The IFBA ZrB_2 coating is treated explicitly. The end plug geometry is modeled as a cylinder, and is similar for fuel rods, WABA rods and control rods. The plenum spring is modeled as a shell of equivalent inner and outer radius and mass. Spacer, mixing, and protective grids are modeled semi-explicitly in KENO, by distributing the grid mass uniformly amongst the 17x17 lattice cells in each assembly slice containing a grid, and placing that mass in an equivalent volume box on the periphery of each cell. Note that there are 8 ZIRLO mixing vane (MV) grids plus 4, shorter, flow mix grids (IFM) within the active fuel height. Inconel top and bottom grids and the protective grid are also modeled. The axial locations of the spacer grids are modeled according to [1]. The mass of the spacer sleeves is incorporated in the grid mass in the model. Figure **7** depicts the KENO spacer grid model. In VERA, each grid and set of sleeves is homogenized locally in the coolant of each assembly axial location containing a grid. The WABA inserts (poison, bottom Zr spacer, and upper plenum), control rods, end plugs, and plenum regions below the top nozzle are modeled explicitly.

Guide tubes and instrument tubes extend from the bottom nozzle to the top nozzle. The structure in the nozzle region is homogenized with the coolant. The dashpot region of the guide tubes is modeled explicitly. Thimble plugs are modeled in the upper regions of the guide tubes which do not contain control or WABA rodlets. The plugs are modeled as solid cylinders with equivalent length to the actual plug. Axially, the model spans the upper and lower core plates, which are homogenized with the coolant in both KENO and VERA, with void boundary conditions outside. Radially the model extends to half the inter assembly gap with reflective boundary conditions outside, and relies on quarter symmetry.

The KENO axial power profile and the % delta nodal power[**] VERA vs. KENO for Assembly 5B (124 IFBA rods with enrichment zoning and axial blankets) is given in Figure 8. The nodal power prediction from VERA agrees very well with KENO except at the grid locations. The discrepancy in the axial levels containing spacer grids, more marked in the shorter ~0.7-in Intermediate Flow Mixing grids (IFM) than in the taller ~2.3-in Mixing Vane (MV) grids is attributable to the approximations underlying the SP_N formulation.

The KENO axial power profile and the % delta nodal power VERA vs. KENO for Assembly 4 (68 IFBA rods, enrichment zoning, 8 long and 4 short WABA inserts, and axial blankets) is given in Figure 9. The top-skewed power distribution is due to the axial asymmetries in the WABA inserts design, which is optimized for HFP MSHIM (rodded) operation. Simulations involving these assemblies at conditions more representative of actual plant operation will be performed in the next Section ("3D 3x3 Multi-Assembly"). It should be noted that the skewed power distribution notwithstanding, the VERA axial power distribution still agrees very well with KENO.

[**] The term "nodal power" here and in the remaining of this paper is used to indicate the power at a given axial location integrated over the pertinent radial plane, in analogy to the terminology used in nodal core simulators. The number of axial planes (or "nodes") at which the comparison is carried out is ~50, as can be seen in Figure 8 and 9.

CASL-U-2015-0006-000

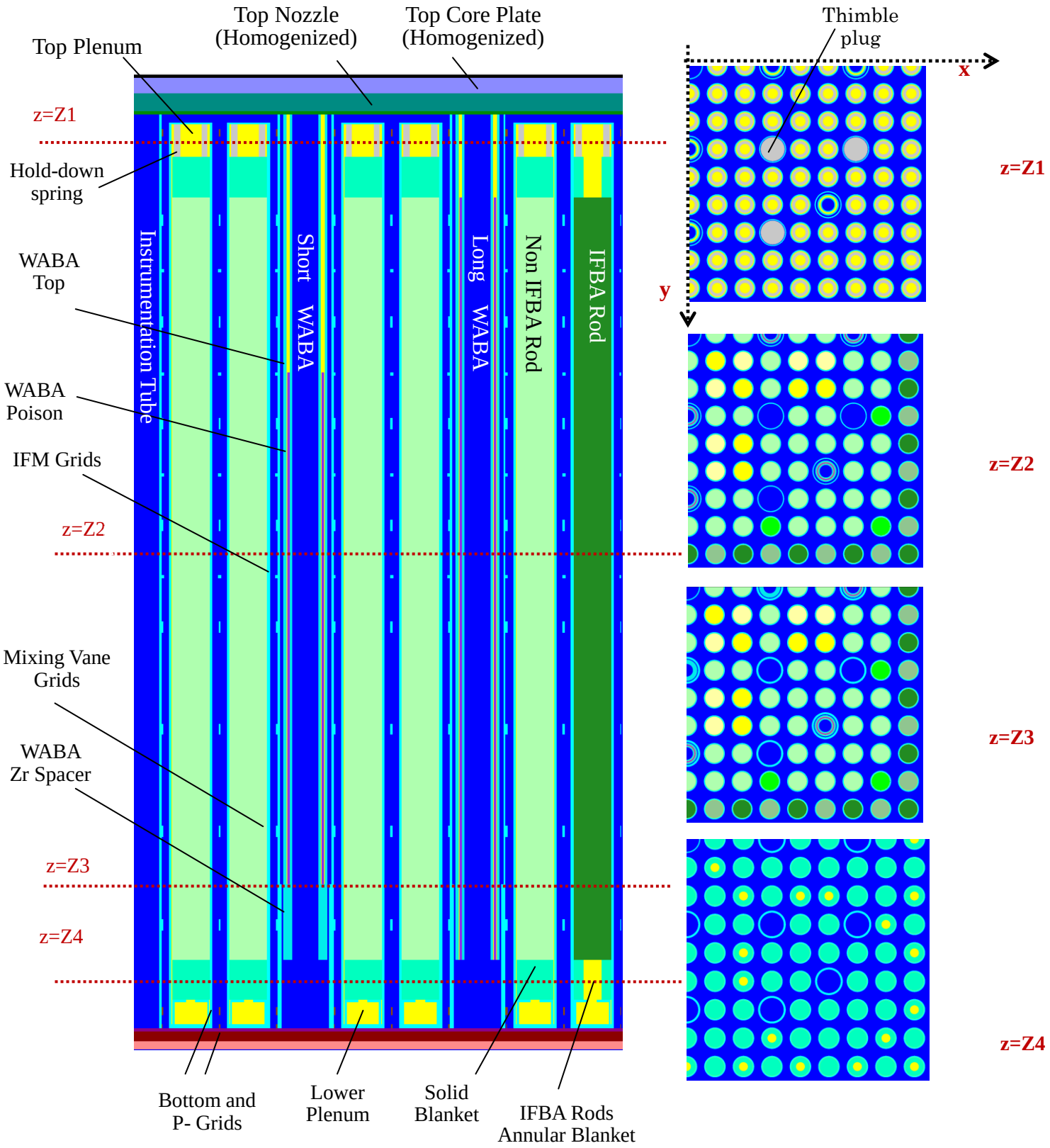

Figure 6 3D Assembly 4 fuel stack model for KENO-VI
(not shown to scale – axial slice at y=0; quarter symmetry)

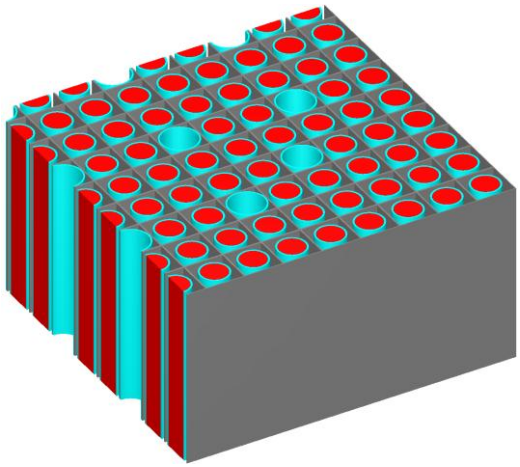

Figure 7 Semi-explicit grid Model in KENO

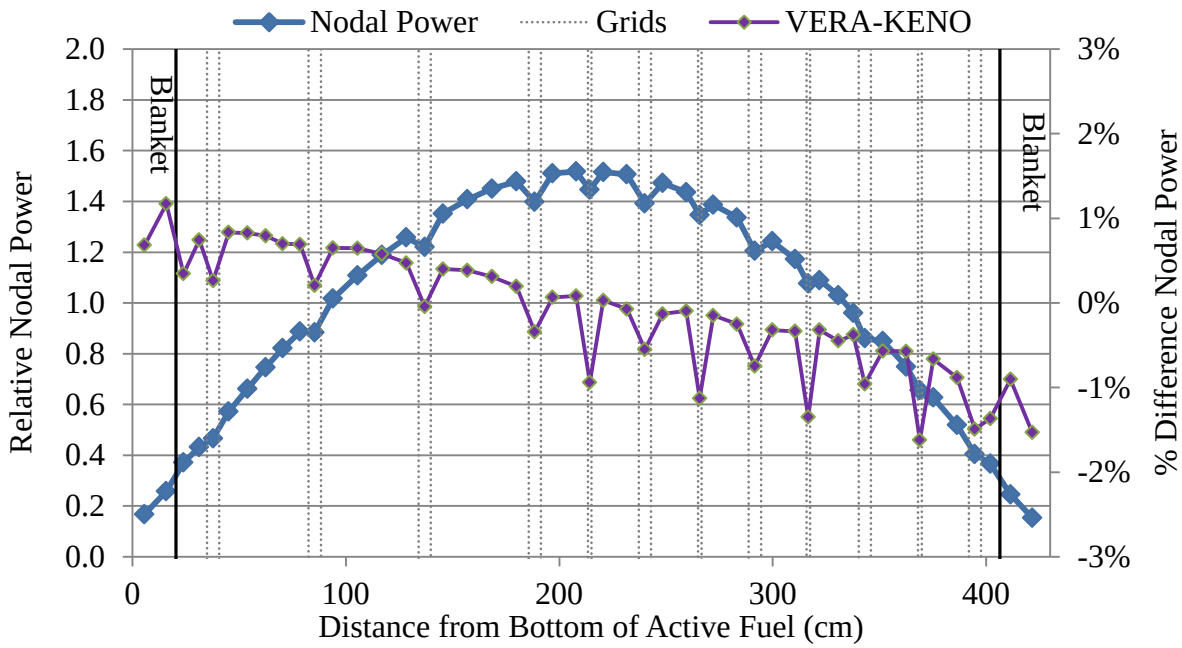

Figure 8 Nodal power for Assembly 5B fuel stack
(124 IFBA, no WABA)

The results for all the assembly simulations performed are summarized in Table 4. Beside reactivity, several figures of merit illustrative of the power distribution agreement between VERA and KENO are shown. The reactivity prediction from VERA remains in excellent agreement with KENO, within 50-100 pcm, showing no significant deterioration with respect to 2D simulations. The natural U assembly, Assembly 1, is within 200 pcm from KENO but this assembly in isolation is subcritical, and it will feature very low power sharing in the core.

The power distribution agreement is overall very satisfactory: the delta Axial Offset (AO) is within 1%, and mostly within 0.5% of VERA. The delta pin power RMS is mostly <0.3%, the 3D delta power RMS calculated over 49 axial planes and 264 fuel rods per assembly is <~0.5% for assemblies where the AO is close to neutral, and ~1% for the assemblies with very positive AO and top-skewed power distribution, caused by the presence of asymmetric WABA inserts as already discussed. The delta power at the hot spot is within 1% for all simulations.

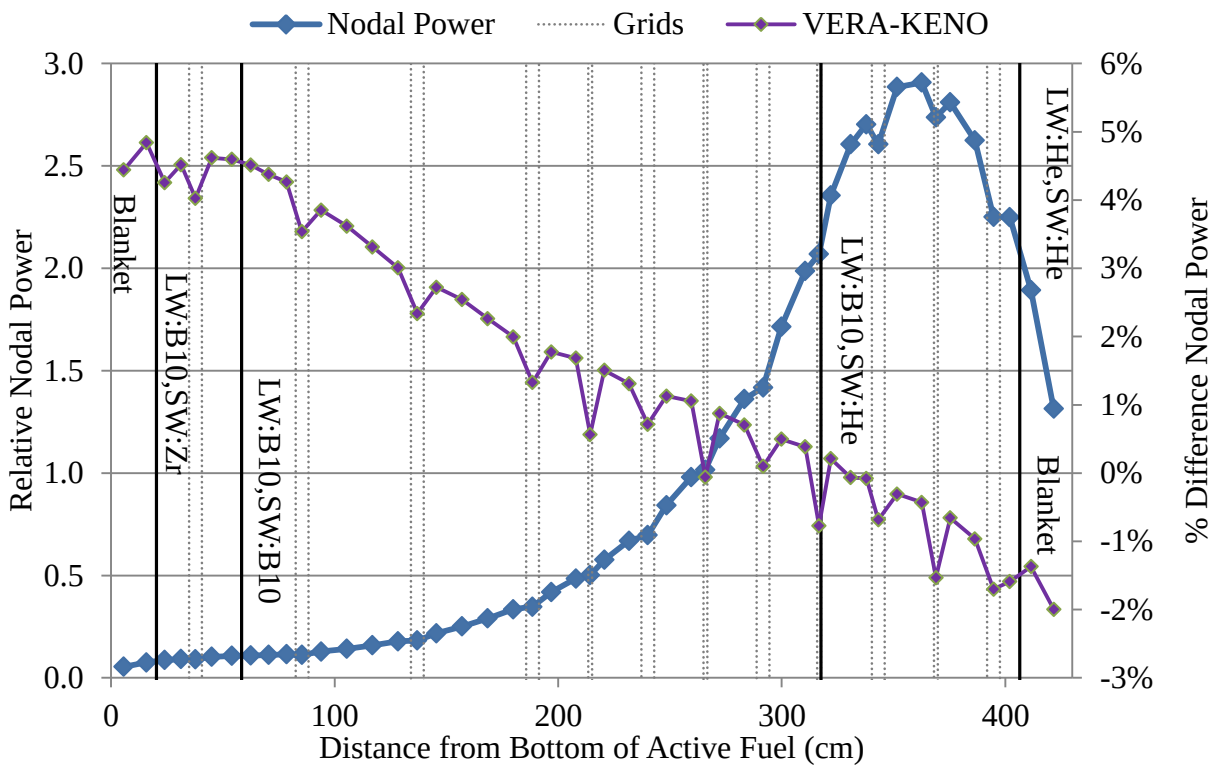

Figure 9 Nodal power for Assembly 4 fuel stack
(68 IFBA plus 8 Long WABA and 4 Short WABA)

Table 4 3 D assembly summary results for all fuel regions

Assembly	K_{eff} (± 1 pcm)	AO (%)	ΔK_{eff} (pcm)	ΔAO (%)	RMS ΔP Pin (%)	RMS ΔP Cell (%)	ΔP Hot Spot (%)
1	0.90409	-2.9	-211	-0.4	0.13	0.47	0.00
2	1.00224	-0.9	-81	-0.2	0.16	0.35	0.19
3	1.00265	1.5	52	-0.3	0.17	0.46	-0.03
4	1.00184	80.9	18	-0.5	0.20	1.29	-0.38
5A	1.00289	53.4	20	-0.8	0.22	1.13	-1.08
5B	1.00317	-0.5	-40	-0.4	0.23	0.54	0.91
5C	1.00225	93.6	-37	-0.2	0.22	1.12	0.97

Note: Soluble boron concentration value was chosen to yield approximate criticality. AO is the Axial Offset, that is the axially integrated nodal power in the top half of the assembly minus the one in the bottom half, normalized by the total integrated value. The "pin" power is the 2D pin-wise axially integrated power. The "Cell" power is the 3D pin-wise power for each fuel rod in the 49 axial layers ("nodes") considered. The "RMS ΔP Pin" is calculated based on the root mean square of the delta pin power (VERA-KENO)×100. The "RMS Cell" is calculated based on the root mean square delta pin power (VERA-KENO)×100 over all the fuel rod locations and axial layers. The "Hot Spot" is the cell with the highest power over the 3D geometry considered. KENO representative uncertainties reported in Table 6.

2.5 3D Multi-Assembly

The results reported in this section refer to a 3×3 multi-assembly simulation, namely the 3D counterpart of the 2D multi-lattice simulation reported in Section 2.2. The KENO model for this simulation is illustrated in Figure 11. The 3x3 assembly arrangement features a checkerboard of Assembly 2 and 4, with a "black" Ag-In-Cd control rod bank inserted in the top portion of the central assembly, Assembly 2. The presence of the control bank counterbalances the effect of the part-length WABA in Assembly 4 fuel and the lack of feedbacks at HZP, enabling to obtain an AO that is approximately neutral. This simulation resembles the operation of the AO Bank, which is inserted in the top of the **AP1000** PWR core and keeps the AO within the prescribed limits during the reactor operation.

The summary results for this simulation are reported in Table 5. As for the previous simulations reported, the eigenvalue prediction is in excellent agreement, -18 pcm for VERA vs. KENO. The agreement in the power distribution is also remarkable, with a <1% delta power RMS over 49 axial levels and 3x3x264 fuel radial positions.

The axial power profile is shown in Figure 11, with the axial transitions in the Assembly 4 WABA inserts displayed using vertical lines. The percent difference in nodal power for VERA-CS vs. KENO is shown on the secondary axis. The difference in the peak node power is less than 1%, and the accuracy in the VERA power profile prediction is only mildly affected by the presence of the partial inserted control rod.

A 3D plot of the power (KENO) and delta power (VERA-KENO) is given in Figure 12. The fuel axial transitions and grid positions in the stack are also shown. Note the power suppression in the top part of the central assembly (Reg.2) from the control rod insertion, which further skews the power to the adjacent Assembly 4 fuel, and downward away from the control rod (see left hand side of Figure 12). The discrepancy in the power prediction at the grids, IFM especially, is visible in the middle and right hand side plots of Figure 12. Also the larger percent difference in delta power in the bottom of the stack is noticeable, which is likely the result of a slight axial tilt in the power profile between VERA-CS and KENO (see also the trend in delta power in Figure 11).

In summary, despite some discrepancy in the power prediction, VERA agrees well with KENO also for this challenging simulation.

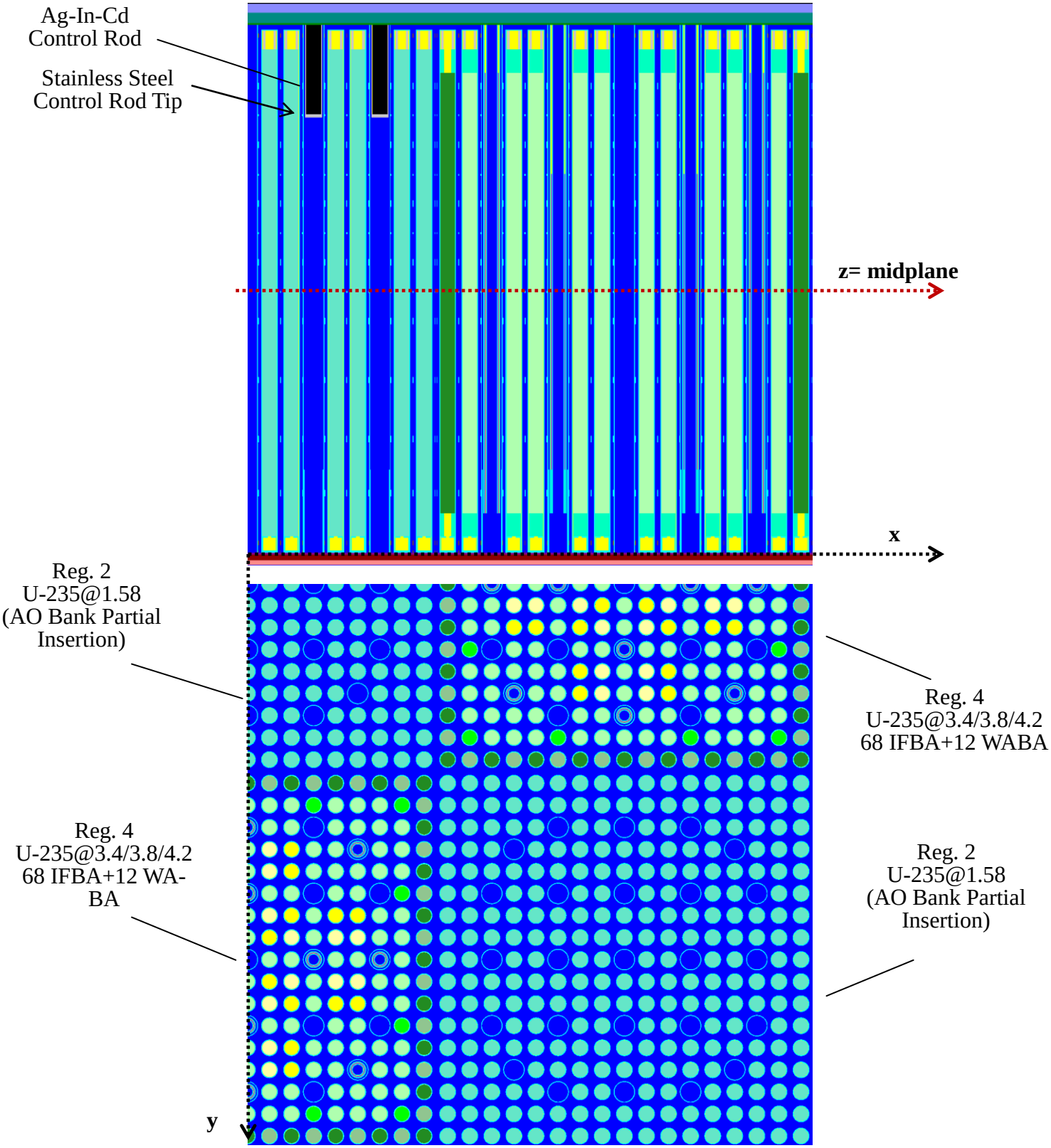

Figure 10 Loading Pattern for Multi-Lattice Simulations
(partial control rod Insertion in central position, Ag-In-Cd "black" bank, 1/4th geometry shown)

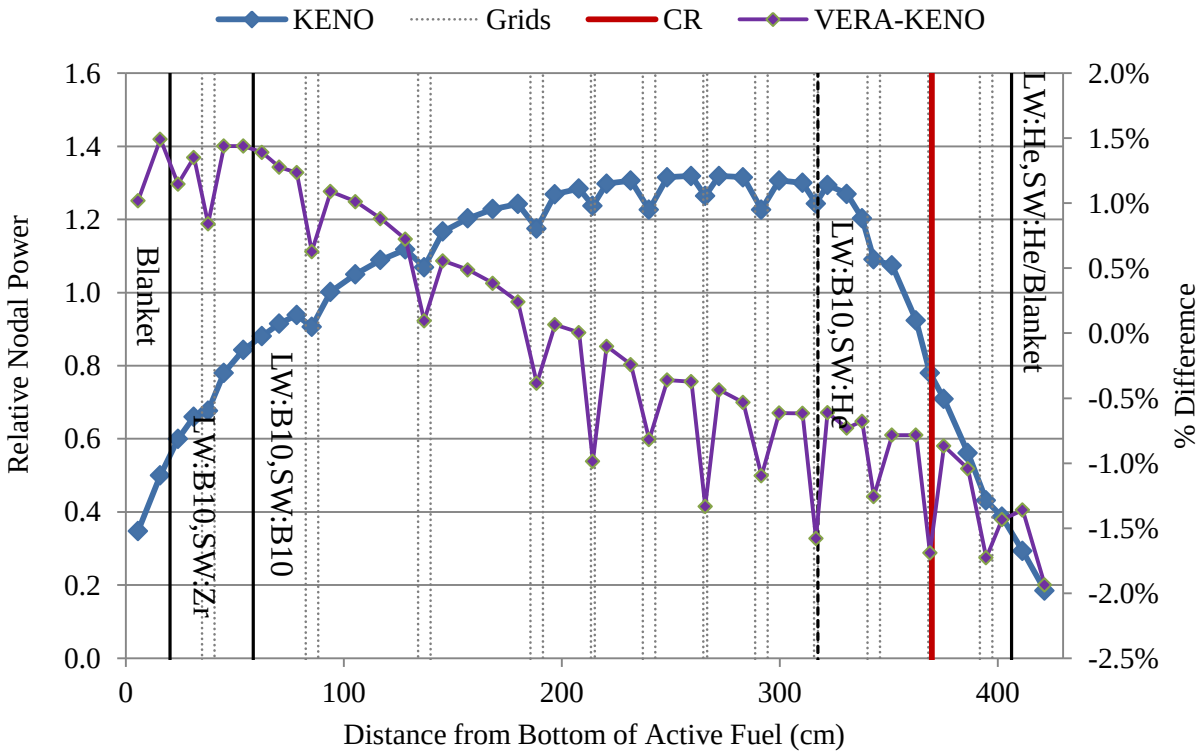

Figure 11 3D 3x3 assemblies axial power distribution with partial insertion of Ag-In-Cd CR (Assembly 2 and 4 with control rod bank in the central assembly)

Table 5 3D 3x3 assembly summary results

KENO		VERA-CS					
K_{eff} (±1 pcm)	AO (%)	ΔK_{eff} (pcm)	Δ AO (%)	RMS/Max ΔP Node (%)	RMS/Max ΔP Pin (%)	RMS/Max ΔP Cell (%)	ΔP Hot Spot (%)
1.00119	2.4	-18	-0.7	0.9/2.1	0.3/0.8	0.9/3.1	-0.3

Note: KENO representative uncertainties reported in Table 6.

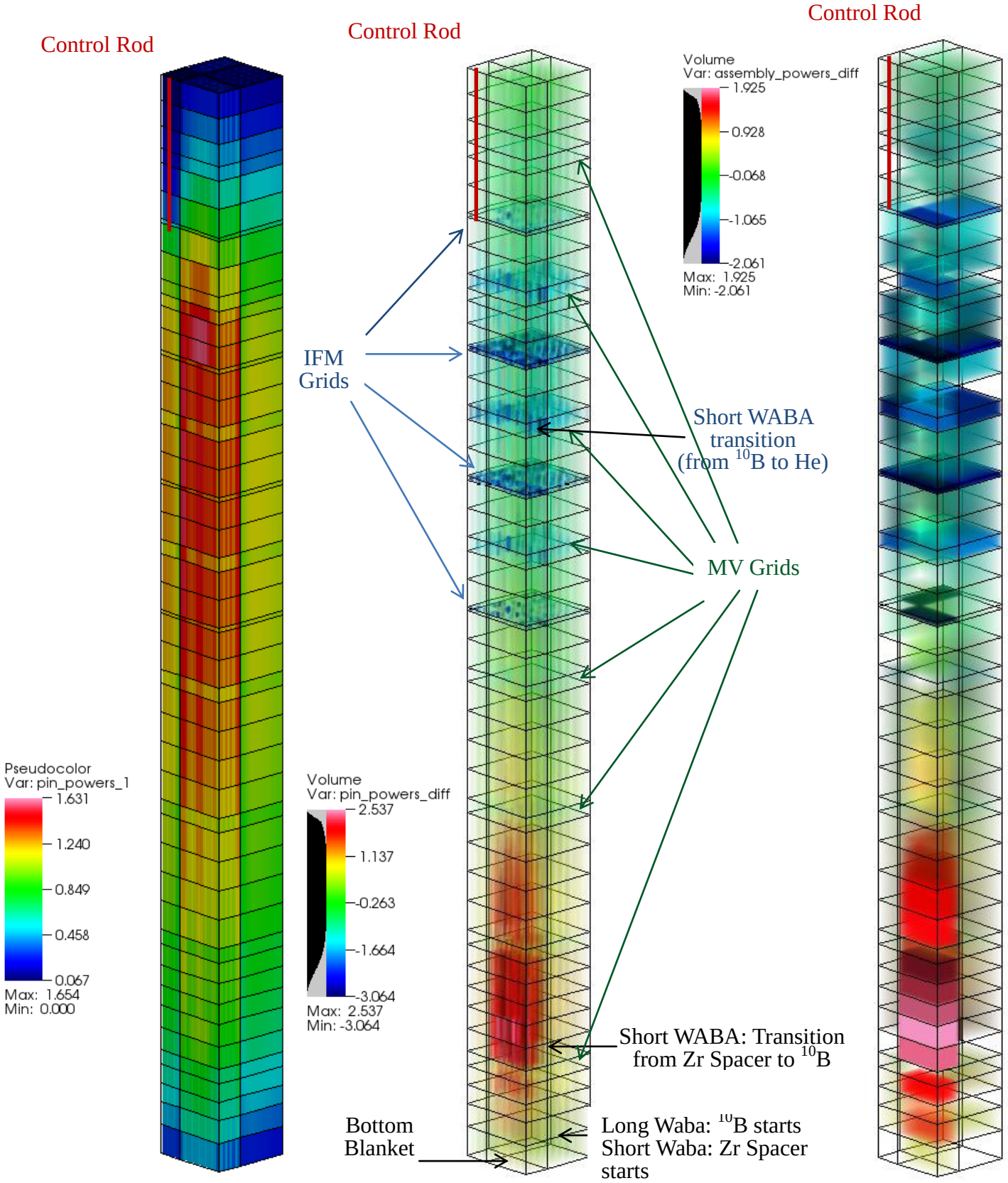

Figure 12 3D 3x3 power (left), delta power VERA-KENO (by cell: middle, by axial node: right)
(Assembly 2 and 4, partially inserted control rod in the central assembly)

3 COMPUTATIONAL RESOURCES

A summary of the computer resources required for performing the VERA-CS and KENO simulations reported is given in Table 6. The VERA-CS simulations have been executed at Westinghouse on a parallel-computation system with 576 cores distributed on 48 nodes, with a total memory of 96 GB/node (8 GB/core). The KENO simulations have been performed on the INL HPC Fission supercomputer.

VERA-CS calculations rely on the SP_5 solver with P_3 scattering and 23 energy groups. Using these options result in relatively low computational resources required for 2D simulations: ~2 min on 12 cores, or ~0.4 core hours, for a 3x3 multi-lattice, ~5 min on 144 cores, or ~13 core hours, for a core radial slice with reflector. 3D simulations become significantly more computationally demanding, especially if fine axial meshes are employed, as it is required to obtain accurate 3D power distributions: a 3D assembly with fine axial mesh structure (~500 axial meshes) results in ~ 200 times the core hours of the corresponding lattice, the 3x3 assembly takes ~ 500 times the core hours of a 3x3 lattice and a 3D core with fine axial meshes (~250 axial layers) takes ~300 times the number of core hours of the 2D core simulation.

A substantial mitigation of the memory requirement and runtime would be required to perform 3D core coupled simulations using the SP_5P_3 23 energy-group flux solver and on-the-fly cross-section generation scheme. It should be noted that the SP_5P_3 solver with 23-energy groups is not the only option available in VERA-CS, and use of a lower SP_N order and/or fewer number of groups to reduce the computation resources is certainly possible. While these alternative options can be further developed and possibly employed in the future for cycle depletion calculations with coupling, the resulting impact on accuracy should be ascertained. At the time of this work the SP_5P_3 with 23 energy groups appeared the most reliable option especially for controlled cases, and has thus been employed.

The KENO calculations have been performed on the INL Fission computer cluster. The 2D lattice simulations rely on 10^9 total particles with 10^6 particles/generation and 100 skipped generations, and were performed on 312 cores, using a memory of 2.7 GB/core. The 2D 3x3 multi-lattice simulations rely on 3.2 10^9 particles, with $2x10^6$ particles/generation and 200 skipped generations, and were performed on 200 cores with 3.2 GB/core. The 2D radial core slice simulation relies on $25x10^9$ particles, with $5x10^6$ particles/generation and 500 skipped generations, and were performed on 300 cores with 5.3 GB/core. The 3D assembly simulations rely on $17.5x10^9$ particles, with $5x10^6$ particles/generation and 500 skipped generations, and were performed on 240 cores with 5.3 GB/core. The 3D multi-assembly simulation relies on $50x10^9$ particles, with $5x10^6$ particles/generation and 500 skipped generations, and were performed on 240 cores with 5.3 GB/core. The resulting statistical uncertainty shown in Table 6 is fairly low and adequate to establish a reference power distribution for comparison to the deterministic VERA results.

In general, KENO requires much larger computational resources than VERA (43,000 core hours for the 2D core vs. 13 in VERA) but it relies on fundamentally different and more general energy and spatial treatments.

Table 6 Computer resources for VERA-CS and KENO simulations

	KENO					VERA-CS				
	Particles (x10^9)	Pin Unc. %	Cores #	Wall Time	Core-hr x10^3	Cores #	Cells #	Core-hr	Wall Time	Memory
2D Lattice	1.1	0.02	312	~3.5h	1	12	324	0.2	~1 min	<96 GB
3x3 Lattice	3	0.04	300	~10h	3	12	3K	0.4	~2 min	<96 GB
2D Core	25	0.06	300	~6d	43	144	86K	13	~5 min	<512 GB
3D Assembly	17.5	0.08	240	~3d	17	64	0.2M	32	30 min	<512 GB
3D 3x3 Assembly	25	~0.1	180	~6d	26	144	1.5M	96	40 min	<1.2 TB

Note: Pin average uncertainty reported.

4 CONCLUSIONS

HZP simulations of the **AP1000** PWR first core have been performed using the CASL core simulator, VERA-CS, with the SP_N solver. In particular, the SP_5 solver with P_3 scattering and 23 energy group pin-cell homogenized cross sections have been used; on-the-fly 1D discrete ordinate transport pin cell calculations with the 252 energy group ENDF/ B-VII.0-based SCALE library are used for the energy and spatial condensation.

The Monte Carlo criticality code KENO-VI with parallel transport capabilities and CE treatment has been used to obtain reference numerical solutions. The KENO simulations rely on an ENDF/B-VII.0 CE cross section library generated by the AMPX code system at the HZP temperature of 565 K.

This paper is focused on the power distribution comparison of VERA and KENO at HZP conditions. VERA shows excellent agreement with KENO for all simulations performed for the **AP1000** PWR first core, an advanced core design featuring radial and axial heterogeneities, IFBA and WABA burnable absorbers, enrichment zoning, and a combination of standard and gray control banks to perform the MSHIM advanced operational strategy. The reactivity prediction from VERA and KENO for geometries from 2D lattice to 3x3 3D multi-assembly and 2D core slices is mostly below 100 pcm. The 3D delta power RMS is typically below 1%, as is the delta power at the hot spot location. The agreement in the power prediction deteriorates in correspondence of the axial grids, in particular for the shorter IFM grids.

Simulations to support 3D core pin power comparisons are currently being performed and the results will be presented in future work.

Computational resources requirements are currently a challenge for VERA and a substantial mitigation is necessary to enable practical cycle depletion simulations [15]. Developments towards this effect are underway.

ACKNOWLEDGMENTS

The authors would like to acknowledge the following individuals for their contribution to this work: Jeff Secker, Dave Salazar, Joel Kulesza, Greg Fischer, Larry Hampshire, Joseph Walsh (Westinghouse), Roscoe Bartlett, Mark Baird (ORNL), the ORNL Insilico development team including Tom Evans, Greg Davidson, and Steven Hamilton, and the SCALE KENO-VI development team including Kursat Bekar and Cihangir Celik, and Ben Collins, Aaron Graham of the University of Michigan.

This research was partially supported by the Consortium for Advanced Simulation of Light Water Reactors (www.casl.gov), an Energy Innovation Hub (http://www.energy.gov/hubs) for Modeling and Simulation of Nuclear Reactors under U.S. Department of Energy Contract No. DE-AC05-00OR22725.

This research used resources of the Oak Ridge Leadership Computing Facility at the Oak Ridge National Laboratory, which is supported by the Office of Science of the U.S. Department of Energy under Contract No. DE-AC05-00OR22725. This research also used resources of the INL High Performance Computing (HPC) Facility at the Idaho National Laboratory.

REFERENCES

[1] M. Hone et al., AP1000 Core Reference Report, Westinghouse Electric Company, March 2012 WCAP-17524-NP

[2] T. Morita, et al., "Application of MSHIM Core Control Strategy for Westinghouse **AP1000** Nuclear Power Plant", GENES4/ANP2003, September 2003.

[3] K. Drudy, etc., Robustness of the MSHIM Operation and Control Strategy in the **AP1000** Design, 17th International Conference on Nuclear Engineering (ICONE 17), July 12-16, 2009, Brussels, Belgium

[4] F. Franceschini, et al., "**AP1000** PWR Reactor Physics Analysis with VERA-CS and KENO-VI – Part I: Zero Power Physics Tests", PHYSOR 2014, Kyoto, Japan, September 28 – October 3, 2014

[5] T.M. Evans et al., 2010. Denovo: A New Three-Dimensional Parallel Discrete Ordinates Code in SCALE. Nuclear Technology, 171, pp.171–200.

[6] SCALE: A Comprehensive Modeling and Simulation Suite for Nuclear Safety Analysis and Design, ORNL/TM-2005/39, Version 6.1, June 2011. Available from Radiation Safety Information Computational Center at Oak Ridge National Laboratory as CCC-785.

[7] E. M. Gelbard, Applications of spherical harmonics method to reactor problems, Tech. Rep. WAPD-BT-20, Bettis Atomic Power Laboratory, 1960.

[8] E. W. Larsen, J. Morel, and J. McGhee, Asymptotic derivation of the simplified PN equations, Proc. ANS Topical Meeting, Mathematical Methods and Supercomputing in Nuclear Applications, 1 (1993), pp. 718-730.

[9] R. G. McClarren, Theoretical aspects of the simplified PN equations, Transport Theor. Stat. Phys., 39 (2011), pp. 73-109.

[10] D.F. Hollenbach, L.M. Petrie, and N.F. Landers, "KENO-VI: A General Quadratic Version of the KENO Program," Vol. II, Sect. F17 of SCALE: A Modular Code System for Performing Standardized Computer Analysis for Licensing Evaluation, NUREG/CR-0200, Rev. 7 (ORNL/NUREG/CR/CSD-2R7), 3 vols., April 2004. Available from the Radiation Safety Information Computational Center at Oak Ridge National Laboratory as CCC-545.

[11] B.T. Reardon et al., "Enhancements in Continuous-Energy Monte Carlo Capabilities for SCALE 6.2", PHYSOR 2014, Kyoto, Japan, September 28 – October 3, 2014.

[12] M.E. Dunn and N.M. Greene, "AMPX-2000: A Cross section Processing System for Generating Nuclear Data for Criticality Safety Applications," Trans. Am. Nucl. Soc. 86, 118–119 (2002).

[13] A. T. Godfrey et al., "Simulation of Watts Bar Unit 1 Initial Startup Tests with Continuous Energy Monte Carlo Methods", PHYSOR 2014, Kyoto, Japan, September 28 – October 3, 2014

[14] J.C. Gehin et al., "Watts Bar Unit 1 Cycle Zero Power Physics Tests Analysis with VERA-CS", PHYSOR 2014, Kyoto, Japan, September 28 – October 3, 2014.

[15] S. Palmtag et al., "Coupled Neutronics and Therma-Hydraulic Solution of a Full Core PWR Using VEA-CS"